biomass

MDPI

Article

Valorization of Algerian Tomato and Hot Pepper Wastes Through Gasification in a Bubbling Fluidized Bed Reactor and Energy Production

Nazim M. Bellal [1,2], Ouacil Saouli [1,2], Massimo Urciuolo [3], Giovanna Ruoppolo [3], Anna Basco [3], Renata Migliaccio [3], Biagio Ciccone [3,4] and Fabrizio Scala [5,*]

[1] Département Génie des Procédés, Ecole Nationale Polytechnique de Constantine, BP 75, A, Nouvelle ville RP, Constantine 25000, Algeria
[2] Laboratoire de Génie des Procédés pour le Développement Durable et les Produits de Santé, Ecole Nationale Polytechnique de Constantine, BP 75, A, Nouvelle ville RP, Constantine 25000, Algeria
[3] Istituto di Scienze e Tecnologie per l'Energia e la Mobilità Sostenibili, Consiglio Nazionale delle Ricerche, Piazzale V. Tecchio 80, 80125 Napoli, Italy; massimo.urciuolo@stems.cnr.it (M.U.); biagio.ciccone@stems.cnr.it (B.C.)
[4] Dipartimento di Scienza Applicata e Tecnologia (DISAT), Politecnico di Torino, Corso Duca degli Abruzzi 24, 10129 Torino, Italy
[5] Dipartimento di Ingegneria Chimica, dei Materiali e della Produzione Industriale, Università degli Studi di Napoli Federico II, Piazzale V. Tecchio 80, 80125 Napoli, Italy
* Correspondence: fabrizio.scala@unina.it

Abstract

This study investigates the potential of tomato waste (TW) and hot pepper waste (HPW) biomass from local food industries in Algeria as sustainable feedstocks for fluidized-bed air gasification. Conversion efficiency, syngas composition and energy content were evaluated under different operating conditions, including gasification temperature (750 and 850 °C) and bed material (silica sand, olivine, and a ZSM-5 zeolite catalyst/silica sand mixture). The results demonstrate that gasification of these biomasses in a bubbling fluidized-bed reactor is an effective waste-valorization route, producing a syngas rich in hydrogen and methane, suitable for power generation and biofuel applications. Under all operating conditions, hot pepper waste generated a syngas with higher energy content than tomato pomace.

Keywords: biomass gasification; food waste valorization; energy; fluidized bed

1. Introduction

Biomass has emerged as a cornerstone of the global transition toward renewable energy, driven by the urgent need for energy security, the mitigation of fossil fuel depletion, and the socioeconomic revitalization of rural regions [1]. In Algeria, the agricultural sector—particularly in the eastern provinces where arable land exceeds 60% of the territory—generates substantial quantities of residues from the food processing industry. Tomato and hot pepper cultivations are of primary importance, with annual waste production estimated at 316 kton and 99 kton, respectively [2]. The alternating harvest seasons (spring–autumn for tomato and autumn–winter for hot pepper) ensure a continuous supply of these residues, commonly referred to as "pomace," throughout the year.

These residues, primarily composed of skins and seeds, present significant disposal challenges due to their high moisture content and rapid biochemical degradation [3,4]. However, their physicochemical properties make them excellent candidates for thermochemical valorization via gasification, pyrolysis, or hydrothermal liquefaction [5].

Received: 3 December 2025
Revised: 16 January 2026
Accepted: 28 January 2026
Published: 6 February 2026

Tomato waste has been widely studied through both experimental and simulation-based approaches [6]. For instance, Hijosa-Valsero et al. used tomato pomace for enzyme-based biofuel production, achieving a 61% saccharification yield from sugar-rich fermentable hydrolysates [7]. Giannelos et al. converted tomato seeds into a heavy bio-oil with low sulfur and ash contents, obtaining a 35% yield on a dry basis for use in a diesel engine [8]. Midhun Prasad et al. produced bio-oil from tomato peels via pyrolysis at temperatures ranging from 450 to 650 °C and heating rates between 5 and 25 °C/min, with subsequent testing in a diesel engine [9]. Elkhalifa et al. examined pyrolysis of several vegetable wastes—tomato, cucumber, carrot, and their blends. Their results showed that blending had minimal effect on CH_4 and H_2 release but significantly influenced CO_2 production. The ternary blend produced a pyro-gas with lower CO_2 concentration compared to individual biomasses, with reductions of 17.10%, 9.11%, and 16.79% for tomato, cucumber, and carrot, respectively [10]. Brachi et al. assessed torrefaction effects on tomato peels, combining experiments with equilibrium modeling, and found that torrefaction only marginally improves product gas quality [11]. In contrast, studies on hot pepper waste are very limited. Furthermore, due to their seasonal complementarity, these residues could be processed alternately in the same decentralized plants; nevertheless, a direct comparative study of their gasification performance is currently missing from scientific literature.

Biomass gasification is a high-temperature (700–1400 °C) thermochemical process that converts organic matter into a combustible 'syngas' (primarily H_2, CO, CH_4 and CO_2) alongside char and tars [12–14]. While steam and oxygen agents favor hydrogen enrichment and higher heating values, air gasification is often preferred for its cost-effectiveness and lower tar yields, despite the resulting nitrogen dilution [15–17]. The process efficiency is governed by parameters such as temperature, particle size, and catalysts, with the equivalence ratio (ER) serving as the critical operational variable in air-blown systems [18–20]. Fluidized bed gasification (FBG) is a leading technology for biomass conversion due to its superior heat and mass transfer rates and precise temperature control [21,22]. Nevertheless, the process is often hindered by the formation of complex tars and the risk of bed agglomeration, particularly when processing ash-rich agricultural residues. The use of active bed materials, such as olivine for tar cracking [23–25] or ZSM-5 zeolites for hydrocarbon enhancement [26,27], offers a promising route to improve syngas quality.

This study addresses the existing literature gap by providing a comprehensive comparative assessment of Algerian tomato waste (TW) and hot pepper wastes (HPW) in a bubbling fluidized bed reactor. The novelty of this work lies in the direct performance comparison of these two feedstocks under identical operating conditions, specifically evaluating the influence of temperature and catalytic bed materials (olivine and ZSM-5) on syngas composition, tar yield, and operational stability, giving insights into the development of decentralized energy systems tailored to the Mediterranean agricultural context.

2. Materials and Methods

The feedstock used for the gasification tests was supplied by a local industry in eastern Algeria and exhibited a non-uniform particle size distribution. Following previous experience and recommendations from the literature [28–30], the biomass was ground and sieved to obtain particles in the 600–710 µm range, which is suitable for feeding into a fluidized bed reactor.

The biomass samples were thoroughly characterized. Proximate analysis was carried out using a LECO TGA701 thermobalance (St. Joseph, MI, USA) according to UNI 9903/ASTM D5142 [31,32] standard procedures. Ultimate analysis was performed with a LECO CHN628 analyzer (St. Joseph, MI, USA) following the ASTM D5373 [33] standard method for determining carbon (C), hydrogen (H), and nitrogen (N). The higher heating

value (HHV) of the biomasses was measured using a Parr 6200 calorimeter (Mardi Gras, IL, USA) following ASTM D5865 [34]. Metal and mineral contents were determined with an Agilent 7500ce (Santa Clara, CA, USA) Inductively Coupled Plasma Mass Spectrometer (ICP-MS) in accordance with the NEN 6427:1999 standard [35]. During gasification, syngas composition was monitored online using an MRU Varioluxx analyzer (Neckarsulm-Obereisesheim, Germany), and the outlet gas was further analyzed with an Agilent 3000A micro-GC (Santa Clara, CA, USA).

Table 1 reports the ultimate and proximate analyses for both tomato pomace and hot pepper pomace. Each analysis was conducted four times, and the mean value was calculated.

Table 1. Ultimate (a.r.) and proximate analysis (a.r.) of the biomass feedstocks.

	Hot Pepper	**Tomato Waste**
Ultimate analysis [%]		
C	42.05	43.71
H	5.80	5.91
N	1.73	2.00
O	50.42	48.39
Proximate analysis [%]		
Moisture	11.66	8.57
Fixed carbon	15.22	12.26
Volatile matter	66.54	73.13
Ash	6.59	6.05
HHV [MJ/kg]	16.98	17.56

a.r.: As received basis.

Multiple materials—namely silica sand, olivine, and a mixture of ZSM-5 zeolite (Si/Al = 40, code 840HOD1A, TOSOH Chemicals, Tokyo, Japan) and silica sand—were used as bed materials in the fluidized bed gasifier. As widely reported in the literature, silica sand is commonly employed due to its availability and low cost. However, under certain conditions, sand beds may undergo agglomeration when interacting with biomass ash [36–38]. Olivine, on the other hand, is known to exhibit a catalytic effect on tar compounds, promoting their cracking and decomposition into non-condensable gases [23–25]. In addition, olivine is less susceptible to agglomeration, making it suitable for biomasses with high ash content. The use of a ZSM-5/sand mixture with a fixed blending ratio has also proven effective. ZSM-5 provides catalytic activity that enhances the formation of hydrocarbons during biomass conversion [26,27].

Figure 1 illustrates the bench-scale experimental apparatus used for the gasification tests. The fluidization column is an electrically heated tubular reactor made of AISI 310 stainless steel, with an internal diameter of 41 mm and a height of 1 m. The column is equipped with a distributor plate made of stainless-steel meshes, which evenly distributes the fluidizing gas across the reactor cross-section, ensuring a well-mixed hydrodynamic regime within the bed. Heating is provided by two half-shell electric ovens connected to a PID controller. A thermocouple and a piezometric pressure transducer were used to monitor the bed temperature and the pressure drop across the reactor, respectively.

To capture elutriated particles—such as fly ash and light char—the reactor outlet is fitted with a metallic filter maintained at 300 °C during operation. The biomass feedstock was introduced laterally into the reactor using a combined pneumatic–mechanical feeding system, as shown in Figure 1.

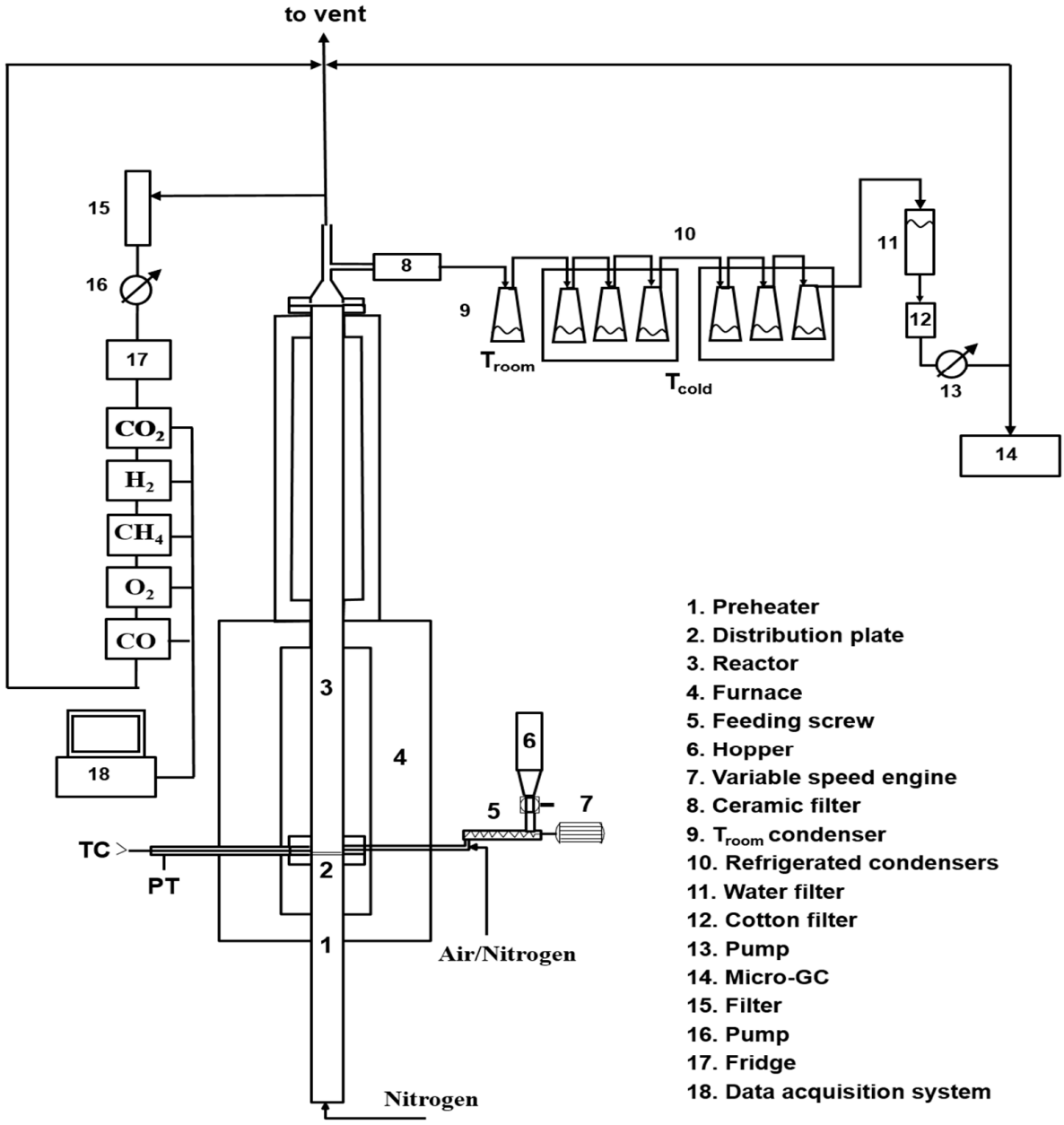

Figure 1. Schematic representation of the bench-scale experimental apparatus.

Before the experimental campaign, the biomass samples were partially dried (to 8.57% moisture for tomato pomace and 11.66% for hot pepper pomace). Gasification of tomato pomace with sand as the bed material proved unfeasible at 850 °C due to the high potassium and sodium content of the tomato waste, which caused bed agglomeration and significantly disrupted reactor performance. Each experiment was carried out for one hour after reaching steady-state conditions in the bench-scale setup. The producer gas was filtered to remove light entrained particles and then passed through a condensation system to separate tars prior to gas analysis. The condensation step consisted of one flask at room temperature followed by a train of three refrigerated flasks at –12 °C to enhance tar recovery for subsequent analysis. After each run, the fluidized bed reactor was cooled to room temperature under an air flow. The reactor bed was then emptied, and the bed material was separated from the char via sieving. Both the bottom ash and the elutriated fly ash were collected and analyzed to determine their composition and properties.

The gasification tests were carried out under the operating conditions reported in Table 2. The bed materials used were silica sand (300–400 μm), olivine (125–180 μm), and a mixture of ZSM-5 zeolite catalyst (300–450 μm) with silica sand, using a zeolite-to-sand blending ratio of roughly 1:3 (26.0% of zeolite by weight). The difference in particle sizes helps maintain proper hydrodynamics in the fluidized bed reactor and facilitates the post-test separation of bed materials through sieving. The total mass of bed material was fixed at 180 g for all tests, in accordance with previous experience showing that this amount ensures a well-developed and well-mixed bubbling fluidization regime.

Table 2. Biomass gasification tests operating conditions.

Test	Biomass	Temperature, °C	Bed Material	ER
1	Hot pepper	750	Sand	0.28
2	Hot pepper	750	Olivine	0.28
3	Hot pepper	850	Olivine	0.33
4	Hot pepper	750	Sand/zeolite	0.25
5	Tomato waste	750	Sand	0.49
6	Tomato waste	750	Olivine	0.52
7	Tomato waste	850	Olivine	0.41
8	Tomato waste	750	Sand/zeolite	0.41

The fluidizing gas consisted of 330 NL/h of nitrogen and 50 NL/h of air. Specifically, 50 NL/h of nitrogen was injected from the bottom of the reactor to generate the bubbling regime, while the remaining 280 NL/h was introduced laterally to assist the pneumatic feeding of biomass particles. An additional 50 NL/h of air was supplied from the bottom, providing approximately 3% oxygen in the fluidizing gas—sufficient to allow partial oxidation of the biomass [39]. The superficial gas velocity was set to Ug = 0.28 m/s, well above the minimum fluidization velocity (Ug $\approx$ 7 U_{mf}).

As previously mentioned, the equivalence ratio (ER) is a key operational parameter in biomass air gasification. It is defined as the ratio of the actual air-to-fuel weight ratio to the stoichiometric air-to-fuel weight ratio required for complete combustion. In this study, the ER ranged between 0.25 and 0.52, which is consistent with the values recommended in the literature for biomass gasification [40].

3. Results and Discussion

3.1. Ultimate and Proximate Analyses

The elemental composition of the investigated feedstocks, specifically in terms of carbon, hydrogen, and nitrogen content, was determined through ultimate analysis. As summarized in Table 1, hot pepper waste (HPW) exhibits a slightly lower carbon content (42.05%) compared to tomato waste (TW) (43.71%), while the hydrogen content is similar for both biomass types (5.80% and 5.91%, respectively). The nitrogen concentration is notably lower in HPW than in TW, which may have favorable implications for reducing NO_x emissions during the conversion process. Oxygen content was determined by difference.

The proximate analysis provides information on moisture, fixed carbon, volatile matter, and ash contents. HPW is characterized by a higher fixed carbon content (15.22%) relative to TP (12.26%), a factor that directly correlates with its superior higher heating value (HHV). Conversely, TP displays a higher volatile matter content (73.13%), suggesting a greater reactivity during the initial stages of devolatilization. The ash content for both biomasses is comparable, ranging between 6.05% and 6.59%.

The mineral profile of the ash, determined via Inductively Coupled Plasma Mass Spectrometry (ICP-MS), is detailed in Table 3. Both feedstocks possess a complex mineral matrix dominated by high concentrations of potassium (K), followed by phosphorus (P), calcium (Ca), and magnesium (Mg). Notably, TW also contains significant quantities of sodium (Na). The high alkali index, particularly the elevated potassium level, is a critical parameter in fluidized bed gasification. In scientific literature, such high K and Na concentrations are frequently associated with the formation of low-melting-point eutectics, which can lead to bed agglomeration and defluidization issues, especially when using silica-based bed materials [36,37].

Table 3. ICP results (as received basis) [ppm].

Metal	Hot Pepper Waste (HPW)	Tomato Waste (TW)
Na	122.60	1697.00
Mg	1772.00	2557.00
Al	100.90	21.58
P	2526.00	1867.00
K	30,320.00	20,070.00
Ca	1089.00	3837.00
Cr	0.73	2.52
Mn	7.65	12.56
Fe	109.30	56.49
Co	0.53	0.20
Ni	0.34	0.42
Cu	5.73	-

3.2. Gasification Tests

Table 4 presents the composition of the syngas at the reactor outlet for each test, calculated on a nitrogen-free basis, while Table 5 reports the calculated gas yield and carbon conversion efficiency for each test. Tests 1 to 4 were carried out using hot pepper waste as the feedstock, whereas tests 5 to 8 correspond to the air gasification of tomato pomace. It can be observed that syngas yield (N_2-excluded) is higher at higher temperatures, and in general carbon conversion efficiency is always higher than 80%. All the O_2 is consumed during the partial oxidation of the fuels and secondary oxidation of volatiles. Syngas composition is sensitive to gasification conditions, especially temperature, ER and the presence of catalysts [41].

Table 4. Syngas composition (N_2-free basis).

Test N°	T [C°]	CO_2 [% vol.]	CO [% vol.]	H_2 [% vol.]	CH_4 [% vol.]	HC * [% vol.]	H_2S [ppm]	HHV [MJ/Nm^3]
Hot pepper waste (HPW)								
1	750	41.93	29.01	17.57	9.67	1.79	19.88	9.7
2	750	35.74	27.64	28.53	7.07	1.02	13.63	9.9
3	850	29.40	33.31	29.54	7.22	0.53	4.13	10.8
4	750	36.38	29.25	24.00	8.65	1.71	5.91	10.2
Tomato waste (TW)								
5	750	47.44	25.56	18.24	6.64	2.12	3.00	8.2
6	750	59.63	18.09	15.86	5.32	1.09	2.76	6.4
7	850	43.23	26.48	22.83	6.26	1.19	1.76	8.7
8	750	49.93	25.23	16.60	6.17	2.07	2.98	7.8

* HC= other light hydrocarbons (ethane, ethylene, propane, propylene).

Table 5. Syngas yield (N_2-free basis) and carbon conversion efficiency (CCE) for each test.

Test N°	Syngas Yield [$Nm^3/kg_{bio\ daf}$]	CCE [%]
Hot pepper waste (HPW)		
1	0.88	88.87
2	0.96	84.27
3	1.19	101.16
4	0.66	61.32
Tomato waste (TW)		
5	0.98	96.06
6	0.82	81.79
7	0.94	85.63
8	0.82	82.03

3.2.1. The Effect of Temperature

The influence of gasification temperature was evaluated exclusively using olivine as the bed material. This choice was necessitated by the bed agglomeration phenomena observed with silica sand at 850 °C, as previously discussed. For hot pepper waste (HPW), elevating the temperature from 750 °C (Test 2) to 850 °C (Test 3) induced a significant shift in the syngas composition: the CO_2 concentration decreased from 35.74% to 29.4%, while the CO content rose from 27.64% to 33.31%. Concurrently, the concentrations of high-energy species increased, with hydrogen (H_2) rising from 28.53% to 29.54% and methane (CH_4) from 7.07% to 7.2%. The observed increase in hydrogen concentration to 28.53 vol.% for HPW at 850 °C is consistent with findings by Mohammed and coworkers [42], who reported a peak H_2 yield of 27.31 vol.% at the same temperature for empty fruit bunch gasification in a fluidized bed. The slightly higher yield in the present study can be attributed to the catalytic role of the olivine bed in promoting secondary cracking reactions, as also suggested by Guo and coworkers [43] regarding the influence of mineral oxides on tar decomposition. As a result of temperature increase, the lower heating value (LHV) of the syngas improved from 9.9 MJ/Nm^3 to 10.8 MJ/Nm^3, in agreement with the literature [44]. A similar trend was observed for tomato waste (TW). Increasing the temperature from 750 °C to 850 °C led to a marked reduction in CO_2 (from 59.63% to 43.23%) and a substantial increase in CO (from 18.09% to 26.48%). Hydrogen and methane concentrations also followed an upward trajectory, reaching 22.83% and 6.26%, respectively. These compositional changes enhanced the syngas heating value from 6.4 MJ/Nm^3 to 8.7 MJ/Nm^3. The different response of the two feedstocks to temperature elevations can be further elucidated by examining their volatile-to-fixed carbon (VM/FC) ratios. Tomato waste (TW), characterized by a higher VM/FC ratio (~5.9) compared to hot pepper waste (HPW) (~4.4), exhibited a more pronounced sensitivity to thermal shifts, in agreement with what was reported by Mohammed et al. [42].

In the context of air gasification, these variations are primarily driven by the temperature dependence of the key thermochemical reactions. The significant reduction in CO_2 accompanied by the increase in CO is largely attributable to the Boudouard reaction ($C + CO_2 \rightleftharpoons 2CO$), which is strongly endothermic and becomes thermodynamically favored at higher temperatures, effectively consuming CO_2 and carbon to produce CO [12–20]. Furthermore, although no external steam was added, the moisture content of the biomass and the water formed during partial oxidation facilitate the water–gas ($C + H_2O \rightleftharpoons CO + H_2$) and water–gas shift ($CO + H_2O \rightleftharpoons CO_2 + H_2$) reactions. At 850 °C, the equilibrium of the water–gas shift reaction shifts toward the reactants, while the endothermic water–gas reaction is promoted, further contributing to the increase in H_2 and

CO [40]. Additionally, higher temperatures enhance the thermal cracking of tars and the reforming of light hydrocarbons, processes that are further assisted by the catalytic activity of olivine [23]. These combined effects lead to a more efficient conversion of biomass into a higher-quality producer gas.

3.2.2. The Effect of Bed Material

The effect of bed material on the air gasification of hot pepper waste can be evaluated by comparing Tests 1, 2, and 4, in which silica sand, olivine, and a sand/ZSM-5 mixture were used, respectively, at a gasification temperature of 750 °C. The results indicate that the incorporation of catalytic materials (olivine and ZSM-5) generally enhances the syngas quality compared to the inert silica sand bed. Specifically, the heating values for the syngas produced with sand, olivine, and the sand/ZSM-5 mixture were 9.7, 9.9, and 10.2 MJ/Nm^3, respectively. This progressive slight improvement in energy content is primarily linked to a reduction in CO_2 concentration and a concomitant increase in high-energy species such as CO and H_2. The observed CO_2 levels are related to the specific equivalence ratio (ER) employed and the varying yields of residual char across the tests. Notably, the hydrogen concentration (on a N_2-free basis) was significantly higher for olivine (28.53%) and the sand/ZSM-5 mixture (24.00%) compared to silica sand (17.57%). For tomato waste (TW) at 750 °C (Tests 5, 6, and 8), the syngas heating values were 8.2, 6.4, and 7.8 MJ/Nm^3, respectively.

The variations in syngas composition and energy yield observed with different bed materials can be fundamentally attributed to the interplay between their catalytic activities and thermal properties. The distinct catalytic nature of the materials significantly influences the secondary gas-phase reactions; for instance, olivine is widely recognized for its effectiveness in promoting the in-situ cracking and reforming of tars, which directly contributes to the increased production of H_2 and CO [23,25]. This catalytic mechanism explains why Test 2 (olivine) yielded the highest hydrogen concentration. In contrast, ZSM-5 zeolite facilitates the deoxygenation of pyrolysis vapors and the formation of light hydrocarbons and aromatics [26,27]. However, the catalytic impact of ZSM-5 was somewhat constrained by its relatively low concentration in the bed (26 wt.%), as higher zeolite fractions were avoided to maintain fluidization stability.

Beyond catalytic effects, the inherent physical properties of the bed materials, such as thermal conductivity and heat capacity, can play role in the heat transfer dynamics within the reactor. Olivine possesses a significantly higher thermal conductivity (typically 3–5 W/m·K, depending on the forsterite content [45]) compared to silica sand (~0.34 W/m·K [46]). This superior thermal property facilitates a more uniform temperature distribution and efficient heat transfer from the reactor walls to the biomass particles, thereby accelerating the endothermic gasification reactions and enhancing overall conversion efficiency. Furthermore, the different particle size distributions and densities of the materials affect the bed's hydrodynamic regime, influencing the gas–solid contact time. These combined catalytic and thermal factors underscore the importance of bed material selection in optimizing the performance of air gasification for agricultural residues like HPW and TW.

3.2.3. HPW and TW: Comparisons

By comparing the results obtained from the two biomasses under the same temperature and bed material conditions, it was observed that the syngas produced from hot pepper waste exhibited a higher heating value than that from tomato pomace (Figure 2).

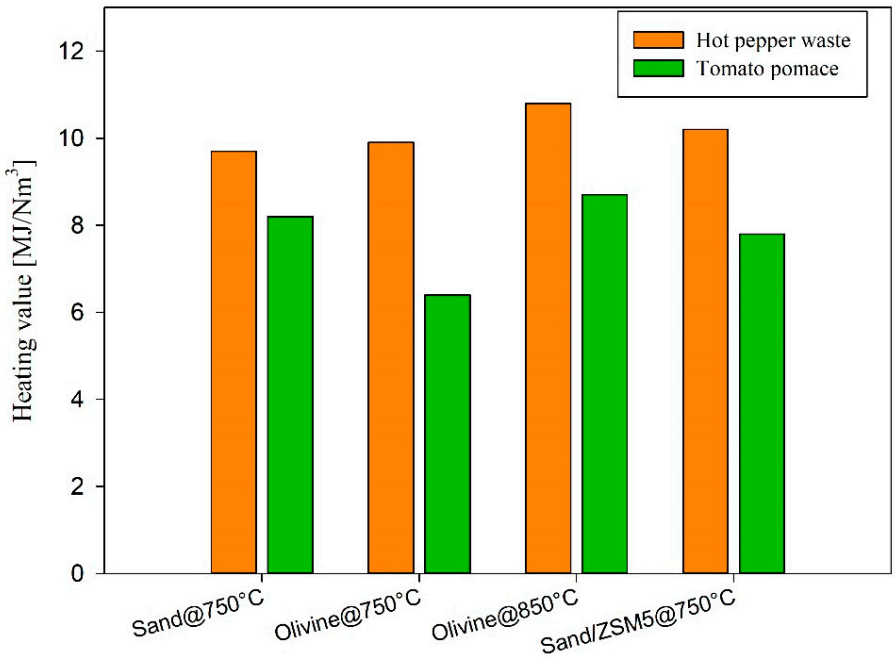

Figure 2. Comparison of syngas heating value for hot pepper pomace and tomato pomace.

The concentration of other light hydrocarbons (HC) in the syngas was determined via gas chromatography, as detailed in Table 6. Ethylene (C_2H_4) was consistently detected in all tests, with concentrations ranging from 0.2% to 1.6%, whereas ethane (C_2H_6) was completely absent. Butane (C_4H_{10}) appeared at negligible concentrations, typically around 0.01%, except in Test 1. Propane (C_3H_8) was more consistently present across the tests, with concentrations ranging from 0.32% to 0.83%. The presence of these species, particularly ethylene, is indicative of the primary cracking of biomass macro-polymers (cellulose, hemicellulose, and lignin) during the devolatilization stage.

Table 6. Concentration of other permanent gases in the syngas.

Test N°	C_2H_4 [% vol.]	C_4H_{10} [% vol.]	C_3H_8 [% vol.]
1	1.13	0.06	0.6
2	0.38	0.01	0.64
3	0.20	0.01	0.32
4	1.29	0	0.42
5	1.60	0	0.52
6	0.25	0.01	0.83
7	0.82	0	0.37
8	1.57	0	0.51

At the end of each experimental run, the char and tars were collected and weighed. Char data are reported in Table 7, while Figure 3 illustrates the tar concentrations in the syngas for both biomass feedstocks. As shown in Table 7, the carbon content in the char derived from HPW (2.31–35.88%) was generally higher than that from TW (2.37–19.4%). For HPW, the transition from silica sand (Test 1) to olivine (Test 2) at a constant equivalence ratio (ER) and temperature resulted in an increase in char carbon content. This trend was further amplified at 850 °C (Test 3) and with the use of the sand/ZSM-5 mixture (Test 4). The higher char carbon levels in these cases may be attributed to the enhanced catalytic activity of the bed, which, while promoting gas-phase reactions and tar cracking, may also facilitate the polymerization of volatile species into secondary char or "coke" on the catalyst surface and within the bed matrix [26].

Table 7. Ultimate analysis of char samples.

Test N°	C [wt.%]	H [wt.%]	Ash [wt.%]
1	2.31	0.22	97.47
2	7.26	-	92.74
3	17.73	0.20	82.07
4	35.88	0.35	63.77
5	19.40	0.24	80.36
6	4.03	0.02	95.95
7	2.37	-	97.63
8	13.41	0.26	86.33

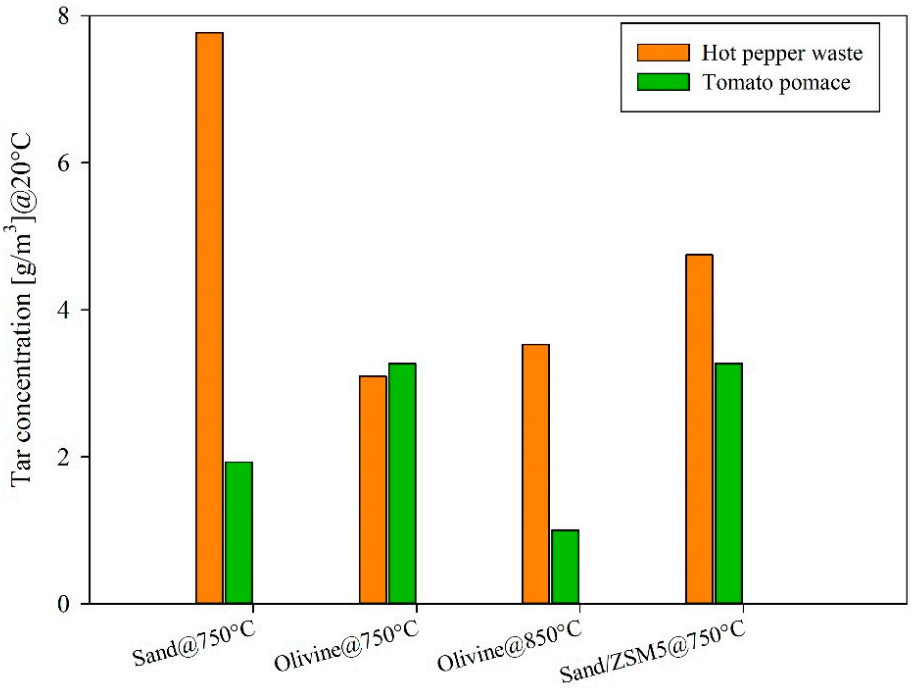

Figure 3. Tar concentration from hot pepper pomace and tomato pomace tests.

Regarding tar production (Figure 3), HPW exhibited higher overall concentrations compared to TW. In line with established literature, the use of olivine significantly reduced tar levels for HPW, confirming its effectiveness as an in-situ catalyst for tar destruction [23,25]. Conversely, TW displayed a different behavior: its syngas consistently contained lower tar concentrations (1–3.27 g/Nm^3), but the introduction of olivine did not yield the expected reduction, even showing a slight increase in some instances. This anomaly might be related to the high alkali content (potassium and sodium) in TW ash, which may interact with the olivine surface, potentially masking its active sites. The observed differences in tar concentration between the two feedstocks can be attributed to their distinct biochemical matrices. A biomass particle undergoes a complex network of chemical reactions during gasification. First, drying and primary pyrolysis (devolatilization) occur, yielding char and volatiles. The latter can then react via oxidation, reforming, cracking, aromatization and other reactions to yield secondary tars [47]. The lower tar yield of TW (1.0–3.27 g/Nm^3) is likely a result of its high volatile content and the presence of endogenous alkali metals (K, Na), which act as internal catalysts for the primary cracking of oxygenated compounds such as phenols and cresols. Conversely, the higher tar levels in HPW syngas suggest a prevalence of more stable tertiary tars, including polycyclic aromatic hydrocarbons (PAHs) like naphthalene. The significant presence of nitrogen in both biomasses (~2 wt.%) further implies that a portion of the condensed tars may consist of nitrogen-containing heterocycles

(e.g., pyridines), which are typical by-products of protein-rich agricultural residues and require specific catalytic strategies for complete removal.

4. Conclusions

This study demonstrates the technical feasibility of valorizing Algerian agricultural residues through fluidized-bed air gasification, identifying specific operational boundaries and performance metrics for hot pepper waste (HPW) and tomato waste (TW). Key results indicate that HPW achieves a superior syngas energy density, with a maximum lower heating value (LHV) of 10.8 MJ/Nm^3 at 850 °C using olivine as the bed material. In contrast, TW produces a syngas with a lower LHV (8.7 MJ/Nm^3) but maintains significantly lower tar concentrations (1.0–3.27 g/Nm^3), which is a critical advantage for reducing the complexity and cost of downstream gas-cleaning units.

The experimental campaign highlighted that while olivine is highly effective for HPW—reducing tar production and increasing hydrogen concentration to 28.53%—its catalytic performance is inhibited when processing TW. This inhibition is directly linked to the high potassium and sodium content in TW ash, which triggers bed agglomeration at 850 °C when using silica sand and likely passivates the active sites of olivine. Furthermore, the use of a ZSM-5 zeolite/sand mixture (26 wt.%) successfully enhanced the syngas LHV for HPW to 10.2 MJ/Nm^3 at 750 °C, demonstrating the potential of specialized catalysts to improve gas quality at lower operating temperatures.

From a practical perspective, these findings provide a quantitative roadmap for the decentralized energy valorization of food processing waste in Algeria. The distinct behaviors of HPW and TW suggest that a flexible gasification strategy—potentially involving the blending of these feedstocks—could balance high energy yield with low tar emissions. Future research should prioritize the development of bed additives or pre-treatment methods to mitigate alkali-induced agglomeration, enabling stable operation at temperatures above 850 °C. Additionally, investigating the long-term stability of ZSM-5 and olivine under real syngas conditions will be essential for scaling up this technology to industrial applications.

Author Contributions: Conceptualization, O.S. and F.S.; methodology, M.U. and G.R.; investigation, N.M.B., A.B., R.M. and B.C.; resources, M.U. and G.R.; data curation, N.M.B. and B.C.; writing—original draft preparation, N.M.B. and B.C.; writing—review and editing, M.U., G.R. and F.S.; supervision, F.S. All authors have read and agreed to the published version of the manuscript.

Funding: This research was funded by the European Union—NextGeneration EU from the Italian Ministry of Environment and Energy Security, POR H2 AdP MMES/ENEA, with involvement of CNR and RSE, PNRR—Mission 2, Component 2, Investment 3.5 "Ricerca e sviluppo sull'idrogeno", CUP: B93C22000630006.

Data Availability Statement: The raw data supporting the conclusions of this article will be made available by the authors on request.

Acknowledgments: The authors are indebted to F. Stanzione for his support in performing ICP-MS analysis on the biomass samples.

Conflicts of Interest: The authors declare no conflicts of interest.

References

1. Saidur, R.; Abdelaziz, E.A.; Demirbas, A.; Hossain, M.S.; Mekhilef, S. A review on biomass as a fuel for boilers. *Renew. Sustain. Energy Rev.* **2011**, *15*, 2262–2289. [CrossRef]
2. Aidat, T.; Benziouche, S.E.; Cei, L.; Giampietri, E.; Berti, A. Impact of Agricultural Policies on the Sustainable Greenhouse Development in Biskra Region (Algeria). *Sustainability* **2023**, *15*, 14396. [CrossRef]
3. Rintu Banerjee, P.B.B. *Valorization of Fruit Processing By-Products*, 1st ed.; Academic Press: Cambridge, MA, USA, 2020.

4. Rosa-Martínez, E.; García-Martínez, M.D.; Adalid-Martínez, A.M.; Pereira-Dias, L.; Casanova, C.; Soler, E.; Figàs, M.R.; Raigón, M.D.; Plazas, M.; Soler, S.; et al. Fruit composition profile of pepper, tomato and eggplant varieties grown under uniform conditions. *Food Res. Int.* **2021**, *147*, 110531. [CrossRef] [PubMed]
5. Sharma, P.; Bano, A.; Singh, S.P.; Atkinson, J.D.; Lam, S.S.; Iqbal, H.M.; Tong, Y.W. Biotransformation of food waste into biogas and hydrogen fuel—A review. *Int. J. Hydrogen Energy* **2022**, *52*, 46–60. [CrossRef]
6. Jeguirim, M.; Khiari, B. Thermochemical conversion of tomato wastes. In *Tomato Processing By-Products*; Academic Press: Cambridge, MA, USA, 2022; pp. 285–332.
7. Hijosa-Valsero, M.; Garita-Cambronero, J.; Paniagua-García, A.I.; Díez-Antolínez, R. Tomato Waste from Processing Industries as a Feedstock for Biofuel Production. *Bioenergy Res.* **2019**, *12*, 1000–1011. [CrossRef]
8. Giannelos, P.N.; Sxizas, S.; Lois, E.; Zannikos, F.; Anastopoulos, G. Physical, chemical and fuel related properties of tomato seed oil for evaluating its direct use in diesel engines. *Ind. Crops Prod.* **2005**, *22*, 193–199. [CrossRef]
9. Midhun Prasad, K.; Murugavelh, S. Experimental investigation and kinetics of tomato peel pyrolysis: Performance, combustion and emission characteristics of bio-oil blends in diesel engine. *J. Clean. Prod.* **2020**, *254*, 120115. [CrossRef]
10. Elkhalifa, S.; Mariyam, S.; Mackey, H.R.; Al-Ansari, T.; McKay, G.; Parthasarathy, P. Pyrolysis Valorization of Vegetable Wastes: Thermal, Kinetic, Thermodynamics, and Pyrogas Analyses. *Energies* **2022**, *15*, 6277. [CrossRef]
11. Brachi, P.; Chirone, R.; Miccio, F.; Miccio, M.; Ruoppolo, G. Entrained-flow gasification of torrefied tomato peels: Combining torrefaction experiments with chemical equilibrium modeling for gasification. *Fuel* **2018**, *220*, 744–753. [CrossRef]
12. Molino, A.; Chianese, S.; Musmarra, D. Biomass gasification technology: The state of the art overview. *J. Energy Chem.* **2016**, *25*, 10–25. [CrossRef]
13. Min, Z.; Asadullah, M.; Yimsiri, P.; Zhang, S.; Wu, H.; Li, C.Z. Catalytic reforming of tar during gasification. Part I. Steam reforming of biomass tar using ilmenite as a catalyst. *Fuel* **2011**, *90*, 1847–1854. [CrossRef]
14. Devi, L.; Ptasinski, K.J.; Janssen, F.J.J.G. Pretreated olivine as tar removal catalyst for biomass gasifiers: Investigation using naphthalene as model biomass tar. *Fuel Process. Technol.* **2005**, *86*, 707–730. [CrossRef]
15. Bhaskar, T.; Balagurumurthy, B.; Singh, R.; Poddar, M.K. Thermochemical Route for Biohydrogen Production. In *Biohydrogen*; Elsevier: Amsterdam, The Netherlands, 2013; pp. 285–316. [CrossRef]
16. Yang, H.; Chen, H. Biomass gasification for synthetic liquid fuel production. In *Gasification for Synthetic Fuel Production: Fundamentals, Processes and Applications*; Elsevier Ltd.: Amsterdam, The Netherlands, 2015; pp. 241–275. [CrossRef]
17. Gil, J.; Corella, J.; Aznar, M.P.; Caballero, M.A. Biomass gasification in atmospheric and bubbling fluidized bed: Effect of the type of gasifying agent on the product distribution. *Biomass Bioenergy* **1999**, *17*, 389–403. [CrossRef]
18. Meng, X.; de Jong, W.; Fu, N.; Verkooijen, A.H.M. Biomass gasification in a 100 kWth steam-oxygen blown circulating fluidized bed gasifier: Effects of operational conditions on product gas distribution and tar formation. *Biomass Bioenergy* **2011**, *35*, 2910–2924. [CrossRef]
19. Hiblot, H.; Ziegler-Devin, I.; Fournet, R.; Glaude, P.A. Steam reforming of methane in a synthesis gas from biomass gasification. *Int. J. Hydrogen Energy* **2016**, *41*, 18329–18338. [CrossRef]
20. Basu, P. Tar Production and Destruction. In *Biomass Gasification Design Handbook*; Elsevier: Amsterdam, The Netherlands, 2010; pp. 97–116. [CrossRef]
21. Migliaccio, R.; Brachi, P.; Montagnaro, F.; Papa, S.; Tavano, A.; Montesarchio, P.; Ruoppolo, G.; Urciuolo, M. Sewage Sludge Gasification in a Fluidized Bed: Experimental Investigation and Modeling. *Ind. Eng. Chem. Res.* **2021**, *60*, 5034–5047. [CrossRef]
22. Liu, Z.; Mayer, B.K.; Venkiteshwaran, K.; Seyedi, S.; Raju, A.S.; Zitomer, D.; McNamara, P.J. The state of technologies and research for energy recovery from municipal wastewater sludge and biosolids. *Curr. Opin. Environ. Sci. Health* **2020**, *14*, 31–36. [CrossRef]
23. Rapagnà, S.; Jand, N.; Kiennemann, A.; Foscolo, P.U. Steam-gasification of biomass in a fluidised-bed of olivine particles. *Biomass Bioenergy* **2000**, *19*, 187–197. [CrossRef]
24. Koppatz, S.; Pfeifer, C.; Hofbauer, H. Comparison of the performance behaviour of silica sand and olivine in a dual fluidised bed reactor system for steam gasification of biomass at pilot plant scale. *Chem. Eng. J.* **2011**, *175*, 468–483. [CrossRef]
25. Virginie, M.; Adánez, J.; Courson, C.; De Diego, L.F.; García-Labiano, F.; Niznansky, D.; Kiennemann, A.; Gayán, P.; Abad, A. Effect of Fe-olivine on the tar content during biomass gasification in a dual fluidized bed. *Appl. Catal. B* **2012**, *121–122*, 214–222. [CrossRef]
26. Lok, C.M.; Van Doorn, J.; Almansa, G.A. Promoted ZSM-5 catalysts for the production of bio-aromatics, a review. *Renew. Sustain. Energy Rev.* **2019**, *113*, 109248. [CrossRef]
27. Buchireddy, P.R.; Bricka, R.M.; Rodriguez, J.; Holmes, W. Biomass gasification: Catalytic removal of tars over zeolites and nickel supported zeolites. *Energy Fuels* **2010**, *24*, 2707–2715. [CrossRef]
28. Hernández, J.J.; Aranda-Almansa, G.; Bula, A. Gasification of biomass wastes in an entrained flow gasifier: Effect of the particle size and the residence time. *Fuel Process. Technol.* **2010**, *91*, 681–692. [CrossRef]
29. Qian, K.; Kumar, A.; Patil, K.; Bellmer, D.; Wang, D.; Yuan, W.; Huhnke, R.L. Effects of biomass feedstocks and gasification conditions on the physiochemical properties of char. *Energies* **2013**, *6*, 3972–3986. [CrossRef]

30. Zhou, J.; Chen, Q.; Zhao, H.; Cao, X.; Mei, Q.; Luo, Z.; Cen, K. Biomass-oxygen gasification in a high-temperature entrained-flow gasifier. *Biotechnol. Adv.* **2009**, *27*, 606–611. [CrossRef]
31. *UNI 9903-10:1992*; Sistemi di Estrazione degli Incondensabili per Condensatori a Superficie—Determinazione delle varie Forme di Cloro Esistenti nel Combustibile. UNI—Ente Italiano di Normazione: Milano, Italy, 1992.
32. *ASTM D5142-02*; Standard Test Methods for Proximate Analysis of the Analysis Sample of Coal and Coke by Instrumental Procedures. ASTM International: West Conshohocken, PA, USA, 2002.
33. *ASTM D5373-21*; Standard Test Methods for Determination of Carbon, Hydrogen and Nitrogen in Analysis Samples of Coal and Carbon in Analysis Samples of Coal and Coke. ASTM International: West Conshohocken, PA, USA, 2021.
34. *ASTM D5865/D5865M-19*; Standard Test Method for Gross Calorific Value of Coal and Coke. ASTM International: West Conshohocken, PA, USA, 2019.
35. *NEN 6427:1999*; Water—Determination of 66 Elements by Inductively Coupled Plasma Mass Spectrometry. NEN (Nederlandse Norm): Delft, The Netherlands, 1999.
36. Ergudenler, A.; Ghaly, A.E. Agglomeration of silica sand in a fluidized bed gasifier operating on wheat straw. *Biornass Bioenergy* **1993**, *4*, 135–147. [CrossRef]
37. Fryda, L.E.; Panopoulos, K.D.; Kakaras, E. Agglomeration in fluidised bed gasification of biomass. *Powder Technol.* **2008**, *181*, 307–320. [CrossRef]
38. Kittivech, T.; Fukuda, S. Effect of bed material on bed agglomeration for palm empty fruit bunch (EFB) gasification in a bubbling fluidised bed system. *Energies* **2019**, *12*, 4336. [CrossRef]
39. Di Lauro, F.; Migliaccio, R.; Ruoppolo, G.; Balsamo, M.; Montagnaro, F.; Imperiale, E.; Caracciolo, D. Tannery Sludge Gasification in a Fluidized Bed for Its Energetic Valorization. *Ind. Eng. Chem. Res.* **2022**, *61*, 16972–16979. [CrossRef]
40. Narvá Ez, I.; Orío, A.; Aznar, M.P.; Corella, J. Biomass Gasification with Air in an Atmospheric Bubbling Fluidized Bed. Effect of Six Operational Variables on the Quality of the Produced Raw Gas. *Ind. Eng. Chem. Res.* **1996**, *35*, 2110–2120. [CrossRef]
41. Alauddin, Z.A.B.Z.; Lahijani, P.; Mohammadi, M.; Mohamed, A.R. Gasification of lignocellulosic biomass in fluidized beds for renewable energy development: A review. *Renew. Sustain. Energy Rev.* **2010**, *14*, 2852–2862. [CrossRef]
42. Mohammed, M.A.A.; Salmiaton, A.; Azlina, W.W.; Amran, M.M.; Fakhru'l-Razi, A. Air gasification of empty fruit bunch for hydrogen-rich gas production in a fluidized-bed reactor. *Energy Convers. Manag.* **2011**, *52*, 1555–1561. [CrossRef]
43. Guo, F.; Dong, Y.; Dong, L.; Jing, Y. An innovative example of herb residues recycling by gasification in a fluidized bed. *Waste Manag.* **2013**, *33*, 825–832. [CrossRef] [PubMed]
44. Ramos, A.; Rouboa, A. Syngas production strategies from biomass gasification: Numerical studies for operational conditions and quality indexes. *Renew. Energy* **2020**, *155*, 1211–1221. [CrossRef]
45. Goes, S.; Hasterok, D.; Schutt, D.L.; Klöcking, M. Continental lithospheric temperatures: A review. *Phys. Earth Planet. Inter.* **2020**, *306*, 106509. [CrossRef]
46. Campanale, M.; Moro, L.; Siligardi, C. Thermal properties of sands and their dependence on physical and environmental factors. *Sci. Rep.* **2025**, *15*, 8352. [CrossRef]
47. Gómez-Barea, A.; Ollero, P.; Leckner, B. Optimization of char and tar conversion in fluidized bed biomass gasifiers. *Fuel* **2013**, *103*, 42–52. [CrossRef]